Heliyon 7 (2021) e06100

Contents lists available at ScienceDirect

Heliyon

journal homepage: www.cell.com/heliyon

Research article

Structural effects of stabilization and complexation of a zinc-deficient superoxide dismutase

Tania M. Manieri [a], Stefano L. Sensi [b,c], Rosanna Squitti [d], Giselle Cerchiaro [a,*]

[a] Center for Natural Sciences and Humanities, Federal University of ABC - UFABC, Avenida dos Estados 5001, Bloco B, 09210-580, Santo André, SP, Brazil
[b] Center for Advanced Studies and Technology - CAST, University G. d'Annunzio of Chieti-Pescara, Italy
[c] Departments of Neurology and Pharmacology, Institute for Mind Impairments and Neurological Disorders – iMIND, University of California - Irvine, USA
[d] IRCCS Istituto Centro San Giovanni di Dio Fatebenefratelli, Brescia, Italy

ARTICLE INFO

Keywords:
Superoxide dismutase
SOD1
Alzheimer's disease
Circular dichroism
Zinc
Copper
ALS
Protein mutation

ABSTRACT

The activity of the erythrocyte Cu_2,Zn_2-superoxide dismutase (SOD1) is altered in Alzheimer's disease (AD) patients. These patients, compared to healthy subjects, exhibit low plasmatic zinc (Zn) levels in the presence of high plasmatic levels of copper (Cu). SOD1 is an antioxidant enzyme characterized by the presence of two metal ions, Cu and Zn, on its active site. On the SOD1, Cu exerts a catalytic role, and Zn serves a structural function. In this study, we generated a modified SOD1 characterized by an altered capacity to complex Zn. The study investigates the metal-binding dynamics of the enzyme, estimating the stability of a SOD1 protein lacking the appropriate Zn site complexation. Our mutant SOD1 possesses a double amino acid mutation (T135S and K136E) that interferes with the correct Zn site complexation. We found that the protein mutations produce unstable Zn coordination and lower enzymatic activity even when complexed with Cu. Analysis with circular dichroism (CD) spectra on metal titration showed a considerable difference between the two Zn entries in the native dimeric enzyme, and Cu presents a simultaneous entrance in the protein. Otherwise, the mutant T135S,K136E-SOD1 exhibited Zn and Cu complexation instability, being a useful in vitro model to study the SOD1 behavior in AD patients.

1. Introduction

A growing body of evidence supports the involvement of trace metals in neurodegenerative disorders such as Alzheimer's disease (AD), the leading cause of dementia in the elderly [1, 2, 3]. In recent years, it has become clear that the dysregulation of the brain metal homeostasis that includes abnormal levels and distribution of copper (Cu), iron (Fe), and zinc (Zn) participates in the AD onset and progression [3]. The lack of homeostasis for these metals and the oxidative consequences of the phenomenon have been extensively investigated in amyotrophic lateral sclerosis (ALS), an oxidative stress-prone neurodegenerative condition in which mutations in Cu_2,Zn_2-superoxide dismutase (SOD1) enzyme occur in the familiar form of the disease and participate in the neurodegenerative process [4]. SOD1 is an antioxidant enzyme that binds Cu or Zn and controls the detoxification of superoxide by converting this neurotoxic species to molecular oxygen and hydrogen peroxide, which is then neutralized to H_2O by the catalase [5, 6]. The role of SOD1 was extensively studied for decades, from its catalytic function discovered by McCord and Fridovich [5], to an enzyme that plays a role not only in free radical detoxification but is also involved in pathological processes [7]. Recently there is a consensus of the enzyme neurotoxicity and its involvement in neurological diseases not only by a simple loss-of-function, as extensively reviewed by Trist et al. [8]. One of the first neurotoxic functions of SOD1 was detected in motor neurons when mutations in the enzyme could lead to ALS [9, 10, 11]. The hypothesis of a SOD1 as a toxic enzyme due to a peroxidase gain-of-function was based on the protein interaction with other oxidant species and formation of free radicals [12, 13], or protein high molecular weight complex production [14] and aggregation of mutant-ALS related SODs [15, 16, 17], instead of being a consequence of SOD1 toxicity itself. SOD is also linked to other neurodegenerative disorders, such as Huntington disease, brain trauma, and inflammation [18].

Meta-analyses show the presence of altered concentrations and distribution of Cu, Fe, and Zn [2, 19, 20] in AD patients, and disrupted Zn metabolism in the brain is linked to neurodegeneration [21]. Changes in metal-binding sites may alter the SOD1 structure and promote enzyme dysfunction. Protein destabilization, leading to protein aggregation, has been proposed as one of the mechanisms in AD [22, 23, 24].

* Corresponding author.
E-mail address: giselle.cerchiaro@ufabc.edu.br (G. Cerchiaro).

https://doi.org/10.1016/j.heliyon.2021.e06100
Received 9 July 2020; Received in revised form 14 January 2021; Accepted 22 January 2021

Levels of SOD1 in AD are inconsistent, as demonstrated by a recent meta-analysis of 15 studies that investigated differences in SOD activity between AD patients and healthy controls [25]. As shown by the study, five studies reported higher SOD1 activity in AD when compared to controls, seven studies showed no difference, and three studies indicated lower activity in AD patients. These variations of SOD activity in AD patients may reflect Cu and Zn variations present in the serum samples. For example, it is known that high Cu levels are present only in 50% of AD patients [26]. Moreover, levels of SOD1 can be altered in AD patients by decreasing the levels of bioavailable Cu with a selective Cu chelating agent such as D-penicillamine, a process that lowers the enzyme activity below control values [27]. With the decline of the activity of this important antioxidant protein, the oxidative stress can be intensified, and the enhanced general oxidative stress was observed in patients with AD. It was found that the intron variant rs2070424 polymorphism of the SOD1 gene is a risk factor for AD [28, 29]. This specific SOD1 polymorphism, although not necessarily related to the metal-binding site, is linked to higher copper concentration and also an impaired risk for Type 2 Diabetes [30] and Parkison disease [31].

Selective Cu chelation has been demonstrated to decrease the SOD1 expression levels in AD patients [27], but the effects of Zn on SOD1 expression or the alteration of the Zn binding sites have not been investigated. Linked to the lower Zn levels found in AD patients and the available information that a single nucleotide polymorphism represents a risk factor for AD, we consider that there is an open link between a SOD1 naturally complexing lower Zn in its structure and an experimental model to study the protein behavior in AD patients. A Zn-deficient SOD1 model could also be useful to study other neurodegenerative diseases in a more sensible approach than simply remove the Zn atom from the protein, as it is pointed that Zn-deficient SOD1 is toxic to motor neurons [32].

To develop a SOD1 that can be useful in further AD studies in vitro and in cellulo, we identified two potential sites of the SOD1 that can interfere with Zn binding and generated a SOD1 mutant enzyme using a site-directed mutation approach to study how the Zn depletion can affect the enzyme structure and its Cu complexation. Specifically, we generated a T135S, K136E mutant SOD1 (Figure 1) to investigate the Cu and Zn SOD1 binding dynamics and elucidate, with circular dichroism (CD) and electron paramagnetic resonance (EPR) spectroscopies, the stability of the enzyme lacking the appropriate Zn complexation site.

2. Methods

2.1. Chemicals

Reagents were purchased from Sigma–Aldrich, Invitrogen, Millipore, Qiagen, Agilent, and Fisher Scientific. Solutions were prepared with distilled water purified using a Millipore Milli-Q system (Millipore, Bedford, MA, USA).

2.2. Construction of the mutated protein

To obtain the mutation of interest, we generated specific primers based on the human SOD1 sequence, available from NCBI (BC001034). The primers were generated according to the protocol established by Quik-Change™ Site-Directed Mutagenesis Kit using the primers below:

5′GGA AAT GAA GAA AGT TCA GAG ACA GGA AAC 3′ *forward.*

3′GTT TCC TGT CTC TGA ACT TTC TTC ATT TCC 5′ *reverse.*

The plasmid pET-3d expressing human native SOD1 (kindly provided by Prof. Joseph S. Beckman of Oregon State University) [33] was inserted into DH5α and BL21 (DE3) pLysS bacteria. The cloned plasmid was then subjected to sequencing to confirm the absence of mutations in the human wtSOD1 gene. The sequencing result was verified in three experimental replicates. Once the plasmid integrity was confirmed by DNA sequencing, the site-directed mutation procedure was started, thereby obtaining the pET-3d plasmid with the new SOD1 that contains the K136E and T135S mutations. The site-directed mutation step followed the protocol established by the Quik Change Site-Directed Mutagenesis kit, Stratagene (Agilient) [34]. All procedures were performed on ice within a laminar flow, ensuring the integrity of the samples and the employed reagents. After confirming the mutation, the plasmid was inserted into competent BL21 (DE3) pLysS bacteria for protein expression. The cDNA sequence of mutated SOD1 has been submitted to GenBank™ by G. Cerchiaro as GenBank accession number MH718438.

2.3. Protein expression

BL21 (DE3) pLysS bacteria, with plasmid pET-3d-SOD1mut or pET-3d-SOD1wt, were grown on plates with solid Luria Broth (LB) medium supplemented with 50 μg/mL Kanamycin. Some of the colonies were selected and grown in liquid LB medium, supplemented with antibiotics. After growth for 14 h, the solution containing the bacteria was

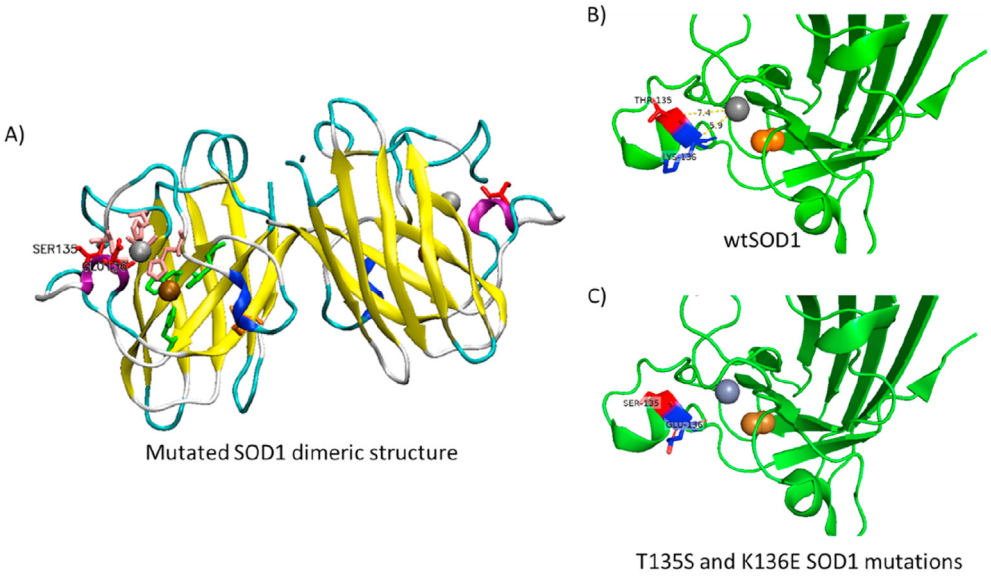

Figure 1. Structure of the human SOD1 (PDC code 2C9V). A) Dimeric structure showing mutated residues, Serine 135, and Glutamic Acid 136, in red; B) wt SOD1 PYMOL simulation with native residues in position 135 and 136; C) mutated SOD1 PYMOL simulation.

centrifuged at 5000 rpm, the supernatant discarded and the pellet suspended in a fresh liquid medium. Bacteria were then adequately stored in aliquots with 50% glycerol in a 1: 1 ratio and frozen immediately.

For protein expression, 100 μL of each bacteria-containing sample was used per liter of liquid Luria Broth (LB) medium. Bacteria were grown under vigorous agitation at 37 °C until an optical density of 0.6–1.0 (0.6 < OD600 < 1.0) was observed. Then, 0.5 mM of IPTG was added to induce protein expression, together with 0.5 mM $CuSO_4$ and 0.5 mM $ZnSO_4$ as copper and zinc sources for SOD1 synthesis. Bacteria were kept at 25 °C for up to 20 h, and the best expression condition was studied. The solution containing the bacteria and proteins was then centrifuged at 5000 rpm, and the pellet was preserved. The pellet resulting from the protein expression was weighed and then suspended in 15 mL of 20 mM Tris-HCl buffer pH 8.0, supplemented with 10 mM NaCl, 2 mM $MgCl_2$, and 1 mL protease inhibitor cocktail P8465 (Sigma-Aldrich) for each 4 g of the bacterial pellet. This solution was subjected to 3 cycles of thermal shock (dry ice + ethanol followed by water bath at 37 °C). After 3 cycles, 1 mg/mL lysozyme was added to produce the rupture of the bacterial membranes, and, after 1 h at room temperature, 10 U/mL benzonase was added for the degradation of RNA and DNA. After 30 min of reaction, the samples were re-metalized, as described in Holo-protein preparation.

2.4. Purification of proteins obtained from plasmid pET-3d

Proteins were pre-purified by saline fractionation and then dialyzed extensively against a 5 mM phosphate buffer pH 8.0 at 4 °C and quantified by absorbance at 280 nm. Samples containing the proteins were then subjected to ion-exchange chromatography, using the ÄKTAprime (GE) equipment fitted with a positive charge RESOURCE ™ Q column, and Tris-HCl 50 mM, pH 8 (A) and Tris-HCl 50 mM, pH 8.0 supplemented with 1.0 M NaCl (B). Purification was carried out with the addition of 1 mL of gradient buffer B sample, 0–100 % in 30 mL, with a flow rate of 0.7 mL/min. From the chromatogram obtained, the fractions that showed peaks at 280 nm, the specific region of the protein, were analyzed by SDS-PAGE to identify the fractions of interest. The human SOD1 (Sigma) was used as the standard for protein weight and for comparison between bands.

2.5. Holo-protein preparation

During protein expression, 100 μL of each sample containing bacteria was used for a liter of liquid Luria Broth (LB) medium. The bacteria grew in vigorous agitation at 37 °C until an optical density between 0.6 and 1.0 (0.6 < OD600 < 1.0) was observed, the exponential phase of bacterial growth. Then, 0.5 mM IPTG was added in order to induce protein expression and 0.5 mM CuSO4 and 0.5 mM $ZnSO_4$ as a source of copper and zinc for the synthesis of Cu, Zn-SOD. The bacteria were at 25 °C for up to 20 h, and the best expression condition was studied. After this period, the solution containing the bacteria and proteins was centrifuged at 5000 rpm, preserving the pellet. The pellet resulting from protein expression was weighed and then resuspended in 15 ml of 20 mM Tris-HCl buffer, pH 8.0, supplemented with 10 mM NaCl, 2 mM $MgCl_2$, and 1 ml of Protease Inhibitor Cocktail P8465 - Sigma-Aldrich) for each 4g of the bacterial pellet. This solution was subjected to 3 cycles of thermal shock, 1 mg/mL lysozyme, and after 1 h at room temperature, 10 U/mL benzonase was added. After 30 min of reaction, the samples were centrifuged at 18000 x g for 10 min at 4 °C. To the supernatant, 0.5 mM $CuSO_4$ and 0.5 mM $ZnSO_4$ were added again, and the mixture was incubated at 4 °C for 14 h. After incubation, the proteins were subjected to thermal precipitation at 65 °C for 30 min. The solution was again centrifuged at 18000 *x g,* and the supernatant recovered.

2.6. Apo-protein preparation

The procedure was done similarly to that described by Rotilio et al. [35]. Both SOD1 and mutated-SOD1 were suspended in a 50 mM potassium phosphate buffer pH 7.5. Thereafter, both proteins were dialyzed separately for 6 h against a sodium acetate buffer 50 mM pH 3.8. The protein was then dialyzed against a 50 mM sodium acetate buffer at pH 3.8 supplemented with sodium 10 mM EDTA for 24 h. The salt replacement was done in the third dialysis against a 50 mM sodium acetate buffer at pH 3.8 plus 0.1 M NaCl for 24 h. Protein samples were finally dialyzed for 24 h against a 50 mM sodium acetate buffer at pH 3.8 and subsequently a 50 mM phosphate buffer at pH 7.4. Once finished the dialysis steps, the protein sample was aliquoted and stored at low temperatures.

2.7. Determination of Cu and Zn in protein samples by flame atomic absorption spectroscopy (FAAS)

To determine the content of Cu and Zn in protein samples, we employed a flame atomic absorption spectrometer – Model AAS Vario 6 (Analytik Jena AG, Jena, Germany) equipped with a hollow Zn or Cu cathode lamp and a deuterium lamp for background correction based on the Zeeman Effect and an automatic sampler. A sliding-bar injector-commutator designed for flow injection analysis was employed to insert the solutions in the FAAS nebulizer. The employed instrumental parameters were: wavelength 231.9 nm, spectral resolution 0.8 nm, current 3 mA, burner height 9 mm, acetylene flow rate 70 L/h, airflow rate 400 L/h. The standard aqueous solutions and certified reference material (CRM or SRM) of the National Institute of Standards and Technology (NIST) 1643e and 1547 were used for reference materials, similarly to described by Bertuchi et al. [36]. The calibration curves for reference solutions were: Cu (5–75 μg/L, Fluka) and Zn (0.25–10.0 mg/L, ULTRA Scientific). All measurements were based on integrated absorbance values.

2.8. Circular dichroism (CD)

The circular dichroism (CD) measurements were done on a Jasco J-815 (JASCO Inc., Tokyo, Japan) spectropolarimeter equipped with a Peltier temperature control PTC-423-S. Samples were prepared at a concentration of 0.5 mg/mL in a 25 mM sodium phosphate buffer at pH 7.4 or KCl 25 mM at pH 7.4, as indicated. All acquisitions were taken in the spectral range of 190–260 nm at 25 °C, using a 0.5 mm quartz cuvette, with a scanning speed of 100 nm/min, a bandwidth of 2 nm, and a response time of 1 s.

2.9. Electronic paramagnetic resonance (EPR)

An additional structural analysis was performed by EPR (EMX 10-2.7 Plus, Bruker). For this assay, 50 μM of protein was used in a solution of water and glycerol 20% (v/v), cooled in liquid nitrogen at 100 K with temperature control, a gain of 4.48×10^4, modulation amplitude: 10 G; power: 20 mW; time constant: 20.48 ms and 4 accumulations.

2.10. SOD activity assays

The SOD activity assay can be performed in a polyacrylamide gel in qualitative analysis [37] or in a spectrophotometer for quantitative analysis [38]. In the gel, samples were added directly to the wells of native polyacrylamide gel and then subjected to 80 V for 15 min and followed by 120 V for 60 min. Gels were then incubated in the dark with a 1.23 mM nitroblue tetrazolium (NBT) solution for 15 min, rapidly washed with water, and incubated with a 100 mM phosphate buffer containing 28 mM TEMED and 2.8 μM riboflavin for 15 min. Gels were washed and subjected to irradiation by a white light for 15 min to initiate the photochemical reaction. In the spectrophotometer analysis, in a

Table 1. Results obtained by FAAS of copper and zinc content on wtSOD1 and T135S,K136E-SOD1 before and after dialysis for metal removal (n = 3).

	Zn/μM	Cu/μM
Holo wtSOD1	3.90 ± 0.15	4.19 ± 0.10
Apo wtSOD1	0.00	0.03 ± 0.001
Holo T135,K136E-SOD1	1.07 ± 0.05	1.21 ± 0.01
Apo T135,K136E-SOD1	0.00	0.00

microtube, it was added the sample volume, corresponding to 10–200 μg of the purified SOD, previously quantified, preferably 20 μg is enough. Then, the volume was completed to 150 μL with 100 mmol/L potassium phosphate buffer solution, with pH adjusted to 7.5; After that, 300 μL NBT 25 mmol/L was added in deionized water and 300 μL riboflavin 2.5 mol/L in 100 mmol/L potassium phosphate buffer solution with pH 7.5 with TEMED [3 μL ([final] = 7 mmol/L); The resulted solution was mixed and exposed to ordinary white light for 30 min with the microtubes open, waiting for 30 min, removed from light and submitted to centrifugation for 15 min (14000 rpm). The supernatant was discarded, and the fine precipitate was resuspended in 1 mL DMF. The absorbance of the sample was measured in a spectrophotometer with a wavelength of 675 nm [38].

3. Results and discussion

Amino acid residues in SOD1 that hydrogen bond to Zn ligands are found within the metal-binding (positions 63, 71, 80, and 83) and electrostatic (positions 124, and 135) loops. The choice of region 136 to play mutations refers that, together with 135, this position is crucial for stabilizing the Zn site in the structure without compromising the SOD1 tridimensional structure. We analyzed the SOD1 structure via VMD (Visual Molecular Dynamics, PDB code 2C9V) to isolate the Zn site and generate a SOD1 that prevents Zn complexation while maintaining the enzyme structural properties (Figure 1A). These two properties, distance, and position are essential for the SOD1 formation since, at physiological pH, lysine is a positively charged amino acid. The T135S and K136E mutations were carried out in conjunction. The objective was to cause a disturbance in the zinc site, not necessarily in the entrance, but mainly its permanence in the site. The monomer of SOD1, when in the absence of Zn ion, the Cu, E-SOD, is a precursor of protein aggregates [39]. It is known that the ZnT3 and ZnT6 zinc transporters have a reduced rate of expression in patients with ALS, and this decrease is not caused by the death of motor neurons [40]. However, the mechanism of the non-allocation of the metal is still unclear. The analysis of the three-dimensional monomeric structure of the protein via PYMOL (Figures 1B and 1C) was based on the isolation of residues close to Zn, with a maximum distance of 8 Å. The analysis showed that both the Lysine residue located at position 136 (K136) and the Threonine residue at position 135 (T135) are at a distance of up to 8 Å from Zn and part of the secondary alpha-helix structure. These two characteristics, distance, and position are important in terms of structural character, and since lysine is a positively charged amino acid at physiological pH, it is believed that its exchange for a negatively charged amino acid, such as glutamic acid, could alter its interaction with Zn, as well as with neighboring

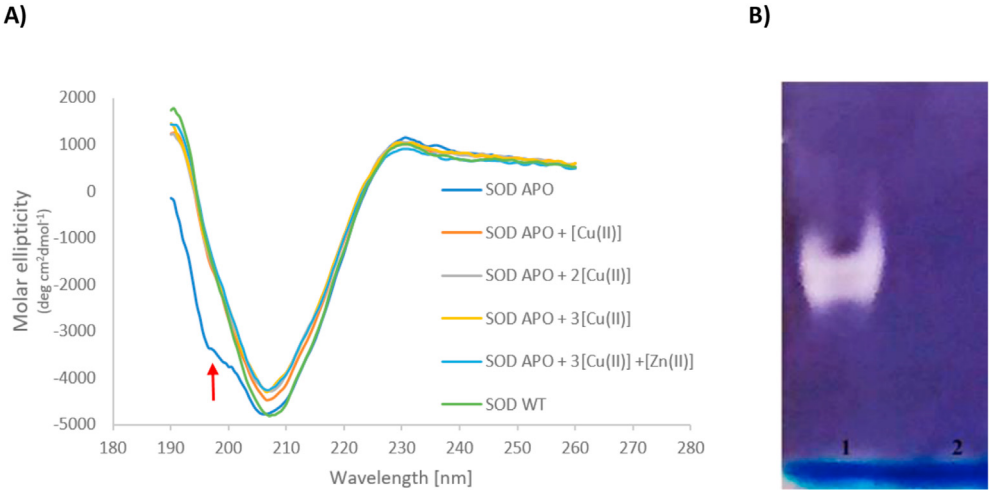

Figure 2. Cu entrance in the SOD1. A) the panel shows the CD spectra of holo-SOD1 and apo-SOD1. The spectra were recorded at a protein concentration of 0.5 mg/mL in 25-mM KCl (pH 7.4) using a 0.5-mm quartz cell at room temperature in the presence of different concentrations of Cu, represented here as molar equivalents. B) SOD1 Nitroblue tetrazolium (NBT) activity gel. Lane 1 shows holo-SOD with regular activity, and lane 2 shows the absence of activity of the apo-SOD1.

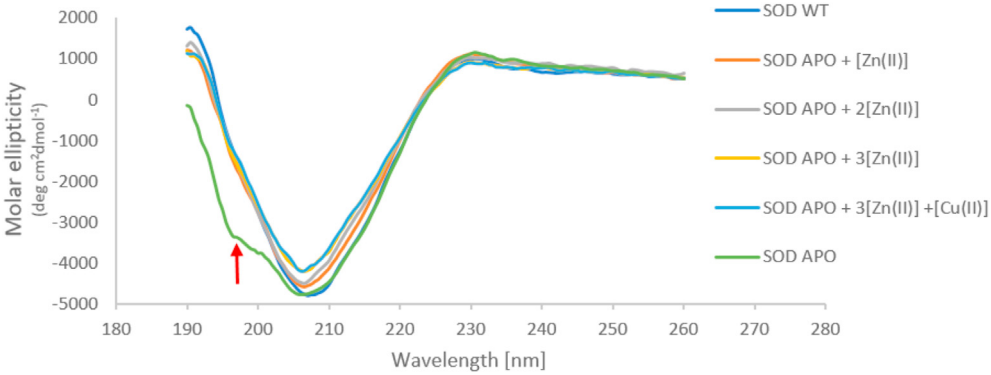

Figure 3. CD spectra of Zn entrance in SOD. The spectra were recorded at a protein concentration of 0.5 mg/mL in 25 mM KCl (pH 7.4) using a 0.5 mm quartz cell at room temperature under titration of different concentrations of Zn, represented here as molar equivalents.

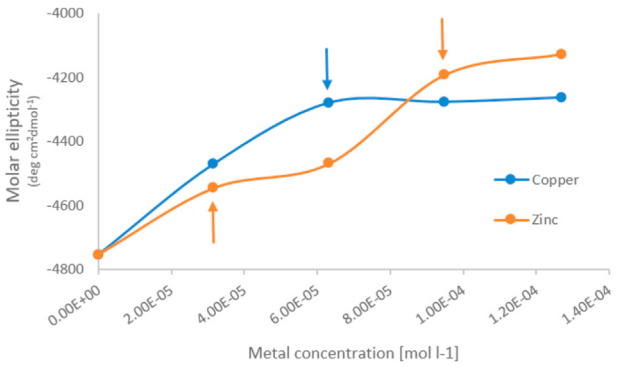

Figure 4. Molar ellipticity Variation at 207 nm. The panel shows the molar ellipticity Variation at 207 nm, which corresponds to the β-barrel region, during the addition of different concentrations of metal ions (M). The blue line shows the apo-SOD treated with Cu stabilized when two equivalents of the metal ion were added. The orange line indicates that the protein was not stabilized even in the presence of Zn in excess. The molar ellipticity values variation was no more than 1–2% in 3 independent experiments, so we presented them in one representative experiment.

amino acids, alternating the geometry of the protein, leading to structural or functional damage, suitable for *in vitro* Zn-deficient SOD1 studies.

After protein expression and purification, it is essential the action of CCS (Copper Chaperone for SOD), a protein found in eukaryotes, for the correct SOD1 metalation [41]. However, the metalation *in vitro* was observed after the protein purification by long time incubation at low temperature, afford the SOD1 expression in prokaryote cell, and also SOD1 metal manipulation [42]. Still, being expressed in bacteria, the protein should not have a properly acetylated N-terminus, a post-translational modification occurring at the SOD1 dimer interface.

Once the expression, purification, and metalation of the native and mutated proteins of interest were confirmed, it was performed the analytical technique FAAS in the Holo (containing all metals) and Apo (after dialysis) forms. The FAAS technique is very accurate when using purified protein in solution [43]. The dialysis successfully produced the apo-forms of the native and T135S,K136E-mutant SOD1. The metal quantification (in Table 1) indicated that the T135S,K136E-SOD1 contains about three to four times less Zn and Cu than found in the native protein.

3.1. SOD1 metal titration by CD

Structural and complexation studies were then carried out on the native and mutant SOD1. At first, the native SOD1 was treated with different concentrations of Cu (Figure 2A) or Zn (Figure 3), and CD spectra were evaluated at each point of the metal titration. The native SOD1 apo-form showed a small deformation in its spectrum in the region of the β-barrel (190–215 nm) (Figures 2A and 3, showed with a red arrow). The region was rapidly restructured with the addition of stoichiometric amounts of Cu or Zn. Figure 2B shows the SOD1 regular activity (white band) in the first lane and the absence of activity of the apo-

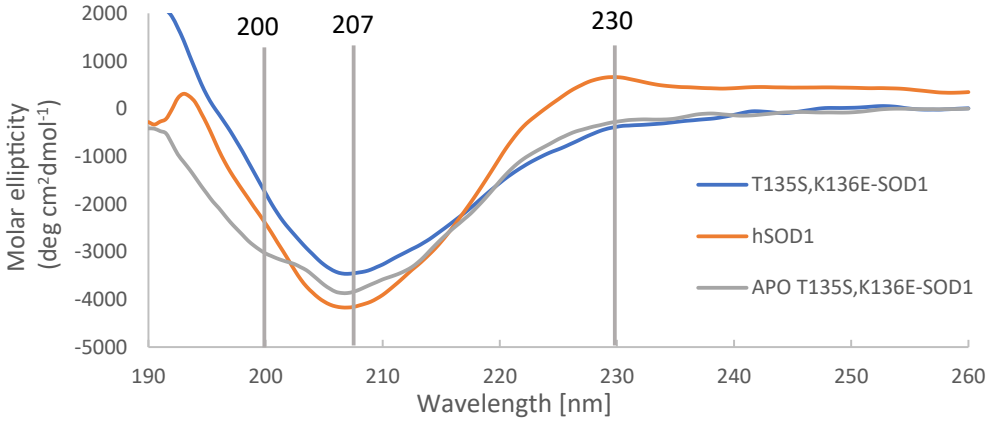

Figure 5. SOD1 CD spectra for T135S,K136E-SOD1 and Apo-T135S,K136E-SOD1 proteins. Each spectrum is the result of 4 accumulations, performed in a quartz cuvette of 0.5 mm optical path, with 0.5 mg/mL protein in 25 mM KCl (pH 7.4).

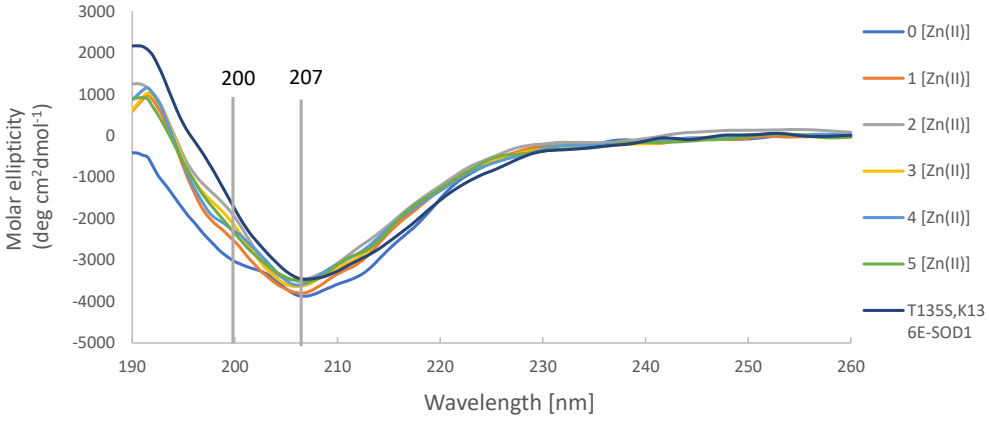

Figure 6. CD spectra of Apo T135S,K136E-SOD1 obtained with the addition of molar equivalents of Zn. Each spectrum is the result of 4 accumulations, carried out in a 0.5 mm quartz cuvette optical path, with 0.5 mg/mL of protein in 25 mM KCl (pH 7.4) at different concentrations of Zn added, and represented here as molar equivalents.

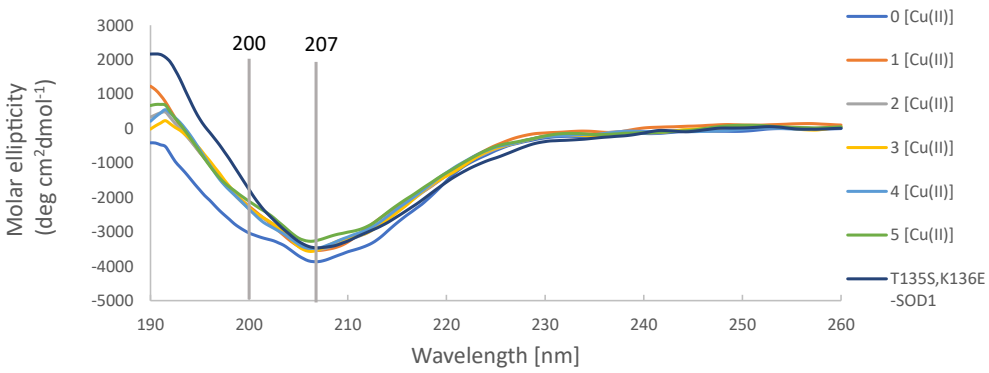

Figure 7. CD spectra for Apo T135S,K136E-SOD1 obtained with the addition of molar equivalents of Cu. Each spectrum is the result of 4 accumulations, carried out in a 0.5 mm quartz cuvette optical path, with 0.5 mg/mL protein in 25 mM KCl (pH 7.4) at different concentrations of Cu, represented here as molar equivalents.

protein in lane 2. In the nitroblutetrazolium (NBT) gel, TEMED reacts with riboflavin to generate superoxide radicals, which react with NBT, thereby producing a deep purple color. The reaction is abolished with physiological SOD activity as O_2 is captured by the enzyme and not able to react with NBT, thereby forming a white band in the gel [37].

With the analysis of apo-SOD1 molar ellipticity of Cu titration, it was assessed the stability of the protein in the 207-nm region after the addition of two equivalents of Cu (Figure 4, blue line, blue arrow). In this case, Cu occupied all the metal sites. However, when the protein was titrated with Zn, the first Zn binding occurred when one metal equivalent was added (Figure 4, orange line) and the second binding with the addition of three equivalents of Zn.

3.2. T135S,K136E-SOD1 structural studies

When performing structural studies, it was observed a maximum decrease in the CD spectrum of T135S,K136E-SOD1 at the 230 nm region (Figure 5 - blue line) compared with the wtSOD1 spectrum (orange line, Figure 5). This phenomenon indicates the presence of a structural change caused by the mutation. The region of the mutated protein is stable even in the absence of metals (Figure 5, grey line).

The absence of metals generated a shoulder in the spectrum at 200 nm that indicates changes in the secondary structure of the mutated protein. This structural change was also seen in the Apo SOD1, thereby suggesting, as previously shown [44], that the absence of the metal produces a local unfolding of the protein. After the addition of the first equivalent of Zn in the apo-T135S,K136E-SOD1, the shoulder at 200 nm disappeared, thereby indicating the restructuration of the protein (Figure 6). The region of 207 nm in this β-sheet-related protein was weakly altered, thereby indicating that the barrel-β region remains stable even after metal removal and replacement (Figure 6).

The analysis was repeated with Cu added to apo-T135S,K136E-SOD1. In this case (Figure 7), the 200 nm minimum region becomes weaker with the addition of Cu equivalents. After the addition of the first Cu equivalent, a return to the Holo-curve at 200 nm minimum region was apparent. The difference in the efficiency of Cu and Zn in restructuring the T135S,K136E-SOD1 can be explained by the high affinity of Zn for the two metal-binding sites of the SOD1. It is known that the binding of the two zinc ions to the SOD1 dimer is thermodynamically asymmetric, meaning that the binding of the first zinc ion to an apo SOD1 exerts more impact on the structure than the binding of the other metal ion [45]. Then, the competition between the metals for the weak Zn binding site of the T135S,K136E-SOD1 was investigated. To this aim, Cu and Zn were added simultaneously (Figure 8). The separate analysis of the 200 nm region showed significant changes in the absence of metals. It was also observed that metals, when added separately, caused an immediate change in the protein structure by molar ellipticity at 200 nm (orange and blue lines, Figure 9A). On the contrary, when metals were added simultaneously, changes were smoother and resulted in an apparent structure equilibrium with the addition of 1 metal equivalent (gray line, Figure 9A).

With the analysis of the molar ellipticity at 207 nm region (Figure 9B), it was noticed that separately added metals caused an abrupt change in the mutated protein. On the other hand, when metals were added simultaneously, the protein presented slow conformational changes (Figure 9B, gray line). The metals exhibit different behavior when interacting separately with a Zn-altered SOD1 in the T135S,K136E-SOD1 protein. However, the mutation in T135S, K136E did not drastically alter the 3D-structure of the enzyme.

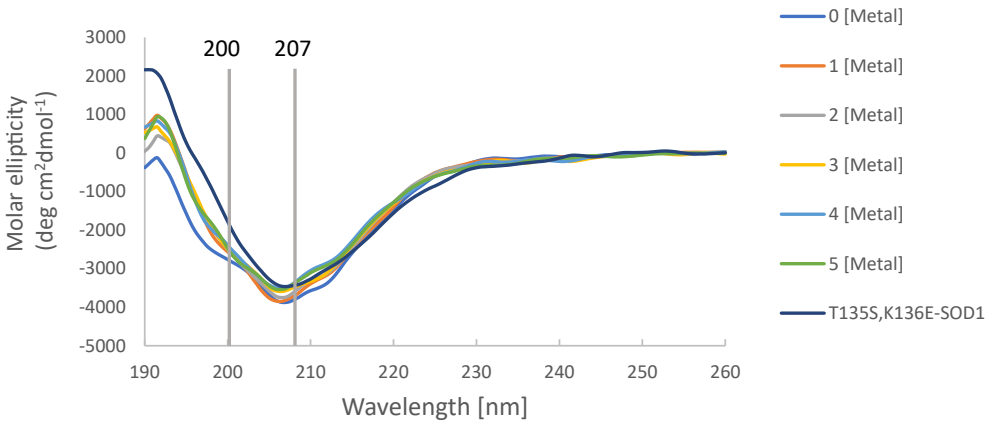

Figure 8. Apo T135S,K136E-SOD1 CD spectra. The panel show CD spectra with both Cu and Zn added, noted as "Metal" in equivalents units. Each spectrum is the result of 4 accumulations, carried out in a 0.5 mm quartz cuvette optical path, with 0.5 mg/mL protein in 25 mM KCl (pH 7.4).

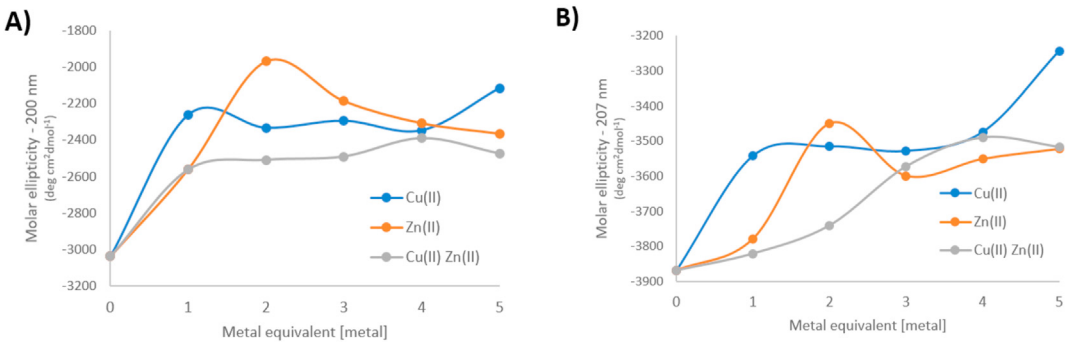

Figure 9. Structural changes of T135S,K136E-SOD1, when different concentrations of metals are added. A) Changes in the 200 nm region; B) Changes in the 207 nm region. The molar ellipticity values variation was no more than 1% in 3 independent experiments, so we presented them in one representative experiment.

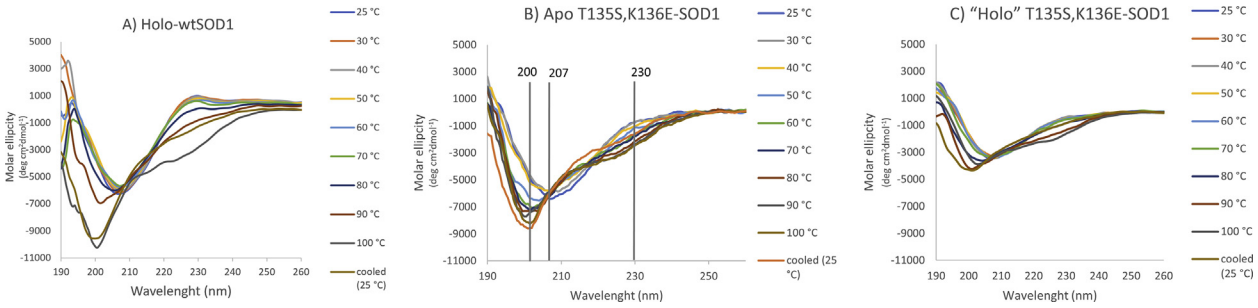

Figure 10. Effect of temperature on the secondary structure of SOD1. Each spectrum is the result of 4 accumulations, performed in a 0.5 mm quartz cuvette optical path, with 0.5 mg/mL protein in a 25 mM phosphate buffer (pH 7.4) at different temperatures. A) Holo-SOD1; B) Apo T135S,K136E-SOD1; C) "Holo" T135S,K136E-SOD1.

It was also measured the thermal stability of the protein in the apo forms of the native and mutated proteins, as well as the metal form. To study the effect of temperature in the mutant T135S,K136E-SOD1, the protein solution was subjected to a heating curve, and a CD spectrum was performed at each new temperature. The thermal stability assay for the Holo-SOD1 (Figure 10A) was performed to verify the method. The results of this set of experiments indicate that SOD1 is robust, undergoes structural destabilization starting at 80 °C, and reaches total destabilization at 90 °C. The T135S,K136E-SOD1 destabilization follows the same temporal profile of the SOD1 (Figure 10B-C) and differs only in the critical temperature that produces the process. The Apo-T135S,K136E-SOD1 protein is more vulnerable, showing a destabilization temperature between 40 and 50 °C, while the Holo-T135S,K136E-SOD1 undergoes destabilization at temperatures in a range between 70 and 80 °C. These data indicate that the T135S, K136E mutation causes a subtle perturbation in the SOD1 structure. However, Cu and Zn always confer stability to the protein, whether native or mutated. Once the stability was established of the mutated protein, the activity of the mutated and native proteins was evaluated. The process was studied, before and after heating, to verify the impact of the mutation on the catalytic site of the enzyme.

Even after using the same amount of protein, T135S,K136E-SOD1 exhibited almost half of the superoxide dismutase activity when compared to the native SOD1 (Figure 10) using nitro blue tetrazolium salt (NTB) in UV-vis spectrometry technique for SOD1 activity quantification [38]. However, considering only the amount of copper in the protein (Table 1), this data leads to conjecture about a possible increase of SOD activity per unit of mutated SOD since the copper/activity ratio will be higher when compared to the wtSOD1. Another important data

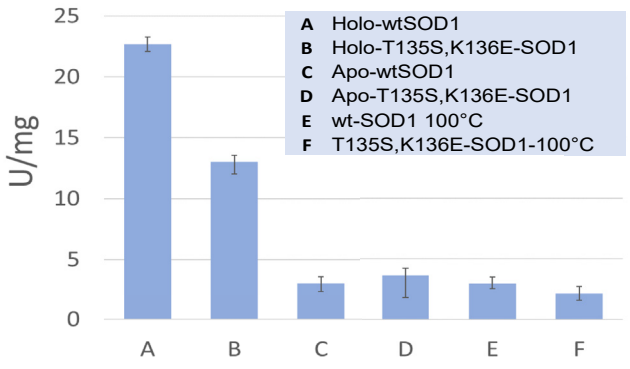

Figure 11. Quantification of SOD activity by NBT method in UV/vis spectrometry, n = 3.

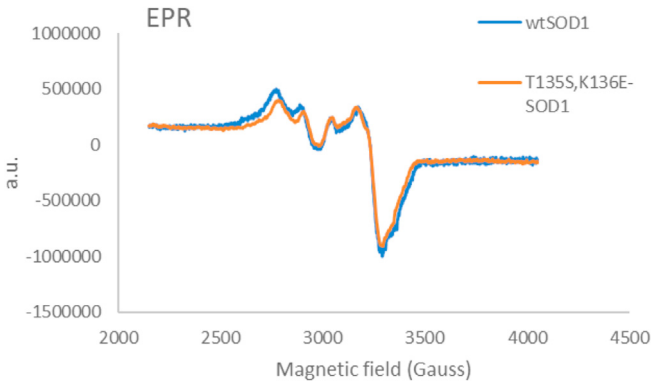

Figure 12. SOD1 electron paramagnetic resonance (EPR) spectra. The panels show the EPR spectrum of wtSOD1 (blue line) and T135S,K136E-SOD1 (orange line). Spectra obtained from 150 μM SOD1 or 570 μM T135S,K136E-SOD1, both diluted in water and glycerol 5% (v/v). Spectra obtained at 100 K with gain of 4.48×10^4, modulation amplitude: 10 G, power: 20 mW, time constant: 20.48 ms, 4 scans.

that can be extracted from Figure 11 (bars C and D) is that the Apo forms of both proteins, whether native or mutant, have no variation in activity, always close to zero. Although the reading of the metal content by FAAS (Table 1) indicates the absence of copper in the samples, in fact, it is that the metal content was below the detection limit of the technique. Thus, a few metal ions that were not chelated during the dialysis are responsible for this basal activity found in apo-protein samples, similarly to control proteins such as human serum albumin. In the same way, basal activity is found in thermally denatured samples at 100 °C (Figure 11, bars E and F).

An electron paramagnetic resonance (EPR) was finally performed to analyze the Cu binding site of the mutated protein (Figure 12). The analysis showed no differences between the spectra of the native and mutated protein, thereby indicating that the mutation had not caused structural changes in the protein's catalytic site. The absence of the Zn complexation site in the T135S,K136E-SOD1 caused an improper Zn entry and blocked part of the Cu entrance. Although it was found 3.8 times less Cu for each SOD1 dimer in the T135S,K136E-SOD1, Cu was still at its correct coordination site in the protein EPR that showed similar *g* factor and *A* hyperfine lines (Figure 12).

High levels of serum Cu and low Zn levels [1, 27] have been reported in AD patients. The imbalance of these essential elements may have effects on the metal supplementation of the SOD1 in erythrocytes and other cells. Our T135S,K136E-SOD mimics this condition, thereby providing insight for further investigations.

4. Conclusions

It was successfully generated a SOD1 variant by producing a double mutation in the amino acids 135 and 136 (T135S,K136E-SOD1). The mutant SOD1 exhibited a correctly structured Cu site, as assessed by EPR spectroscopy, but presented an unstructured Zn site. The Cu and Zn SOD1 binding dynamics were evaluated in a condition that mimics a state of Zn deficiency. The results of these experiments indicated that the absence of Zn in the enzyme generated a poor SOD antioxidant activity and a structural destabilization of the enzyme. CD spectra data showed that the mutated protein did not display changes in its barrel-β and maintained part of its catalytic activity, although structural changes caused by the mutation affected the entrance of Cu and Zn. The mutant SOD1 analyzed here differed from the well-known H43R-SOD1 [46], as its mutations were done in the amino acids directly linked to Zn, thereby mimicking *in vitro* a condition of decreased bioavailability of this metal. The results showed deleterious effects on SOD1 function and stability when the protein had a low capacity to bind Zn. On a speculative note, these data can be interpreted in the context of pathological conditions like AD where Zn depletion occurs. These findings suggest that a defective Zn complexation concur to increase the oxidative stress by the weakening of the antioxidant activity of a Zn deficient SOD1.

Declarations

Author contribution statement

Giselle Cerchiaro: Conceived and designed the experiments; Performed the experiments; Analyzed and interpreted the data; Contributed reagents, materials, analysis tools or data; Wrote the paper.

Tania M Manieri: Performed the experiments; Analyzed and interpreted the data; Contributed reagents, materials, analysis tools or data; Wrote the paper.

Stefano L Sensi: Analyzed and interpreted the data; Wrote the paper.

Rosanna Squitti: Analyzed and interpreted the data; Contributed reagents, materials, analysis tools or data; Wrote the paper.

Funding statement

This work was supported by the Fundação de Amparo à Pesquisa do Estado de São Paulo (FAPESP,2018/14152-0, 2012/24604-0 and 2019/14350-0), Conselho Nacional de Desenvolvimento Científico e Tecnológico (CNPq) and Coordenação de Aperfeiçoamento de Pessoal de Nível Superior (CAPES, financial code 001). Rosanna Squitti and Stefano L Sensi were supported by the Alzheimer's Association (Part the Cloud: Translational Research Funding for Alzheimer's Disease (PTC), PTC-19-602325).

Data availability statement

Data will be made available on request.

Declaration of interests statement

The authors declare the following conflict of interests: Rosanna Squitti; [R. Squitti is Chief Scientific Officer at IGEA PharNV.V. and has shared from IGEA PharNV.V].

Additional information

No additional information is available for this paper.

Acknowledgements

We thank the Multiuser Central Facilities (CEM) at Federal University of ABC for the use of the CD and EPR.

References

[1] M. Ventriglia, G.J. Brewer, I. Simonelli, S. Mariani, M. Siotto, S. Bucossi, et al., Zinc in Alzheimer's disease: a meta-analysis of serum, plasma, and cerebrospinal fluid studies, J Alzheimer's Dis. 46 (1) (2015) 75–87.

[2] D.D. Li, W. Zhang, Z.Y. Wang, P. Zhao, Serum copper, zinc, and iron levels in patients with Alzheimer's disease: a meta-analysis of case-control studies, Front. Aging Neurosci. 9 (SEP) (2017) 1–13.

[3] S.L. Sensi, A. Granzotto, M. Siotto, R. Squitti, Copper and zinc dysregulation in alzheimer's disease, Trends Pharmacol. Sci. [Internet] 39 (12) (2018) 1049–1063.

[4] D.R. Rosen, T. Siddique, D. Patterson, D.A. Figlewicz, P. Sapp, A. Hentati, et al., Mutations in Cu/Zn superoxide dismutase gene are associated with familial amyotrophic lateral sclerosis, Nature 362 (6415) (1993) 59–62.

[5] J.M. McCord If, Superoxide dismutase. An enzymic function for erythrocuprein (hemocuprein), J. Biol. Chem. 244 (22) (1969) 6049–6055.

[6] I. Fridovich, Superoxide radical and superoxide dismutases, Annu. Rev. Biochem. 64 (1) (1995) 97–112.

[7] J.M. McCord, M.A. Edeas, SOD, oxidative stress and human pathologies: a brief history and a future vision, Biomed. Pharmacother. 59 (4) (2005) 139–142.

[8] B. Trist, J.B. Hilton, P.J. Crouch, D.J. Hare, K.L. Double, Superoxide dismutase 1 in health and disease: how a front-line antioxidant becomes neurotoxic, Angew. Chem. Int. Ed. (2020). In press.

[9] M.E. Gurney, H. Pu, A.Y. Chiu, M.C. Dal Canto, C.Y. Polchow, D.D. Alexander, et al., Motor neuron degeneration in mice that express a human Cu,Zn superoxide dismutase mutation, Science (80-) 264 (5166) (1994) 1772–1775.

[10] A.G. Reaume, J.L. Elliott, E.K. Hoffman, N.W. Kowall, R.J. Ferrante, D.F. Siwek, et al., Motor neurons in Cu/Zn superoxide dismutase-deficient mice develop normally but exhibit enhanced cell death after axonal injury, Nat. Genet. 13 (1) (1996) 43–47.

[11] J.S. Valentine, P.A. Doucette, S. Zittin Potter, Copper-zinc superoxide dismutase and amyotrophic lateral sclerosis, Annu. Rev. Biochem. 74 (1) (2005) 563–593.

[12] H. Ischiropoulos, L. Zhu, J. Chen, M. Tsai, J.C. Martin, C.D. Smith, et al., Peroxynitrite-mediated tyrosine nitration catalyzed by superoxide dismutase, Arch. Biochem. Biophys. 298 (2) (1992) 431–437.

[13] E.F. Healy, A. Roth-Rodriguez, S. Toledo, A model for gain of function in superoxide dismutase, Biochem. Biophys. Reports [Internet] 21 (November 2019) (2020) 100728.

[14] J.A. Johnston, M.J. Dalton, M.E. Gurney, R.R. Kopito, Formation of high molecular weight complexes of mutant Cu,Zn-superoxide dismutase in a mouse model for familial amyotrophic lateral sclerosis, Proc. Natl. Acad. Sci. U. S. A. 97 (23) (2000) 12571–12576.

[15] P.B. Stathopulos, J.A.O. Rumfeldt, G.A. Scholz, R.A. Irani, H.E. Frey, R.A. Hallewell, et al., Cu/Zn superoxide dismutase mutants associated with amyotrophic lateral sclerosis show enhanced formation of aggregates in vitro, Proc. Natl. Acad. Sci. U. S. A. 100 (12) (2003) 7021–7026.

[16] L.I. Bruijn, M.K. Houseweart, S. Kato, K.L. Anderson, S.D. Anderson, E. Ohama, et al., Aggregation and motor neuron toxicity of an ALS-linked SOD1 mutant independent from wild-type SOD1, Science (80-) 281 (5384) (1998) 1851–1854.

[17] J.I. Niwa, S.I. Yamada, S. Ishigaki, J. Sone, M. Takahashi, M. Katsuno, et al., Disulfide bond mediates aggregation, toxicity, and ubiquitylation of familial

amyotrophic lateral sclerosis-linked mutant SOD1, J. Biol. Chem. 282 (38) (2007) 28087–28095.
[18] C.M. Maier, P.H. Chan, Role of superoxide dismutases in oxidative damage and neurodegenerative disorders, Neuroscientist 8 (4) (2002) 323–334.
[19] R. Squitti, R. Ghidoni, I. Simonelli, I.D. Ivanova, N.A. Colabufo, M. Zuin, et al., Copper dyshomeostasis in Wilson disease and Alzheimer's disease as shown by serum and urine copper indicators, J. Trace Elem. Med. Biol. [Internet] 45 (October 2017) (2018) 181–188.
[20] M. Schrag, C. Mueller, U. Oyoyo, M.A. Smith, W.M. Kirsch, Iron, zinc and copper in the Alzheimer's disease brain: a quantitative meta-analysis. Some insight on the influence of citation bias on scientific opinion, Prog. Neurobiol. [Internet] 94 (3) (2011) 296–306.
[21] M.P. Cuajungco, G.J. Lees, Zinc metabolism in the brain: relevance to human neurodegenerative disorders, Neurobiol. Dis. 4 (3–4) (1997) 137–169.
[22] G. Torsdottir, J. Kristinsson, J. Snaedal, S. Sveinbjörnsdóttir, G. Gudmundsson, S. Hreidarsson, et al., Case-control studies on ceruloplasmin and superoxide dismutase (SOD1) in neurodegenerative diseases: a short review, J. Neurol. Sci. [Internet] 299 (1–2) (2010) 51–54.
[23] K. Murakami, N. Murata, Y. Noda, S. Tahara, T. Kaneko, N. Kinoshita, et al., SOD1 (copper/zinc superoxide dismutase) deficiency drives amyloid β protein oligomerization and memory loss in mouse model of Alzheimer disease, J. Biol. Chem. 286 (52) (2011) 44557–44568.
[24] G. Rotilio, K. Aquilano, M.R. Ciriolo, Interplay of Cu,Zn superoxide dismutase and nitric oxide synthase in neurodegenerative processes, IUBMB Life 55 (10–11) (2003) 629–634.
[25] M. Schrag, C. Mueller, M. Zabel, A. Crofton, W.M. Kirsch, O. Ghribi, et al., Oxidative stress in blood in Alzheimer's disease and mild cognitive impairment: a meta-analysis, Neurobiol. Dis. [Internet] 59 (2013) 100–110.
[26] S. Brenner, R. Squitti, D. Lupoi, P. Pasqualetti, G. Dal Forno, F. Vernieri, et al., Elevation of serum copper levels in Alzheimer's disease [3] (multiple letters), Neurology 60 (9) (2003) 1559.
[27] L. Rossi, R. Squitti, P. Pasqualetti, E. Marchese, E. Cassetta, E. Forastiere, et al., Red blood cell copper, zinc superoxide dismutase activity is higher in Alzheimer's disease and is decreased by D-penicillamine, Neurosci. Lett. 329 (2) (2002) 137–140.
[28] K. Spisak, A. Klimkowicz-Mrowiec, J. Pera, T. Dziedzic, A. Golenia, A. Slowik, rs2070424 of the SOD1 gene is associated with risk of alzheimer's disease, Neurol. Neurochir. Pol. [Internet] 48 (5) (2014) 342–345.
[29] Y. Li, C. Ma, Y. Wei, Relationship between superoxide dismutase 1 and patients with Alzheimer's disease, Int. J. Clin. Exp. Pathol. 10 (3) (2017) 3517–3522.
[30] J. Yin, X. Wang, S. Li, Y. Zhu, S. Chen, P. Li, et al., Interactions between plasma copper concentrations and SOD1 gene polymorphism for impaired glucose regulation and type 2 diabetes, Redox Biol. [Internet] 24 (December 2018) (2019) 101172.
[31] C. Liu, J. Fang, W. Liu, Superoxide dismutase coding of gene polymorphisms associated with susceptibility to Parkinson's disease, J. Integr. Neurosci. 18 (3) (2019) 299–303.
[32] J.S. Beckman, A.G. Estévez, J.P. Crow, L. Barbeito, Superoxide dismutase and the death of motoneurons in ALS, Trends Neurosci. 24 (11 Suppl) (2001) 15–20.
[33] B. Leinweber, E. Barofsky, D.F. Barofsky, V. Ermilov, K. Nylin, J.S. Beckman, Aggregation of als mutant superoxide dismutase expressed in Escherichia coli, Free Radic. Biol. Med. 36 (7) (2004) 911–918.
[34] H. Liu, J.H. Naismith, An efficient one-step site-directed deletion, insertion, single and multiple-site plasmid mutagenesis protocol, BMC Biotechnol. 8 (2008) 91.
[35] G. Rotilio, L. Calabrese, F. Bossa, D. Barra, A.F. Agrò, B. Mondovì, Properties of the apoprotein and role of copper and zinc in protein conformation and enzyme activity of bovine superoxide dismutase, Biochemistry 11 (11) (1972) 2182–2187.
[36] F.R. Bertuchi, R. Papai, M. Ujevic, I. Gaubeur, G. Cerchiaro, General chelating action of copper, zinc and iron in mammalian cells, Anal. Methods 6 (21) (2014) 8488–8493.
[37] C. Chen, S. Pan, C.N. Chen, S. Pan Sdp, Assay of superoxide dismutase activity by combining electrophoresis and densitometry, Bot. Bull. Acad. Sin. (Taipei) 37 (2) (1996) 107–111.
[38] Giselle Cerchiaro, Tania Maria Manieri, Larissa Lago, S.C. Bianca Dempsey, BR10201600321,Patent: Detection and Quantification Od SOD in a Fast and Economic Kit, 2015.
[39] S. Nedd, R.L. Redler, E.A. Proctor, N.V. Dokholyan, A.N. Alexandrova, Cu,Zn-superoxide dismutase without Zn is folded but catalytically inactive, J Mol Biol [Internet] 426 (24) (2014) 4112–4124.
[40] M. Kaneko, T. Noguchi, S. Ikegami, T. Sakurai, A. Kakita, Y. Toyoshima, et al., Zinc transporters ZnT3 and ZnT6 are downregulated in the spinal cords of patients with sporadic amyotrophic lateral sclerosis, J. Neurosci. Res. 93 (2) (2015) 370–379.
[41] V.C. Culotta, L.W.J. Klomp, J. Strain, R.L.B. Casareno, B. Krems, J.D. Gitlin, The copper chaperone for superoxide dismutase, J. Biol. Chem. 272 (38) (1997) 23469–23472.
[42] L. Banci, I. Bertini, F. Cantini, M. D'Onofrio, M.S. Viezzoli, Structure and dynamics of copper-free SOD: the protein before binding copper, Protein Sci. 11 (10) (2009) 2479–2492.
[43] G. Cerchiaro, T.M. Manieri, F.R. Bertuchi, Analytical methods for copper, zinc and iron quantification in mammalian cells, Metallomics 5 (10) (2013) 1336–1345.
[44] F. Kitamura, N. Fujimaki, W. Okita, H. Hiramatsu, H. Takeuchi, Structural instability and Cu-dependent pro-oxidant activity acquired by the apo form of mutant SOD1 associated with amyotrophic lateral sclerosis, Biochemistry 50 (20) (2011) 4242–4250.
[45] S.Z. Potter, H. Zhu, B.F. Shaw, J a Rodriguez, P a Doucette, S.H. Sohn, et al., Binding of single zinc Ion to subunit of Cu-Zn superoxide dismutase apoprotein substantially influence structure stability of the entire homodimer, J. Am. Chem. Soc. [Internet] 129 (1) (2007) 4575–4583.
[46] N. Fujimaki, F. Kitamura, H. Takeuchi, Pro-oxidant copper-binding mode of the apo form of ALS-linked SOD1 Mutant H43R denatured at physiological temperature, Biochemistry 52 (31) (2013) 5184–5194.